Furin-Mediated Intracellular Self-Assembly of Olsalazine Nanoparticles for Enhanced MR Imaging and Tumor Therapy

Yue Yuan[1], Jia Zhang[2], Xiaoliang Qi[1], Guanshu Liu[2], Xiaolei Song[1], Michael T. McMahon[2], and Jeff W.M. Bulte[1,2]

[1]The Russell H. Morgan Department of Radiology and Radiological Science; Cellular Imaging Section and Vascular Biology Program, Institute for Cell Engineering, The Johns Hopkins University, Baltimore, MD, United States.
[2]F.M. Kirby Center for Functional Brain Imaging, Kennedy Krieger Institute, Baltimore, MD, United States.

Introduction

CEST MRI holds great promise for biomedical applications and molecular diagnostics. There is, however, a lack of enzyme-activatable probes for cancer-specific imaging. Furin is a pro-protein convertase that activates many cancer development-related substances such as growth factors, growth factor-receptors, adhesion molecules, and is overexpressed in malignant tumor cells[1]. We report here on a new molecular probe Olsa-RVRR, in which the exchangeable hydroxyl protons in olsalazine provide CEST contrast with the cell-penetrating peptide RVRR acting as a specific substrate for furin. After the Olsa-RVRR enters furin expressing cells, the RRVR peptide is cleaved by furin, initiating a condensation reaction between the GSH-induced 1,2-aminothiol group and the cyano group of the 2-cyanobenzothiazole motif, resulting in the formation of olsalazine nanoparticles (Olsa-NPs) with exchangable groups on the surface. As it has been reported that cancer cells can be killed by the DNA methylation inhibitor olsalazine[2], we investigated whether intracellular assembly of Olsa-NPs could represent new theranostic approach.

Schematic Outline

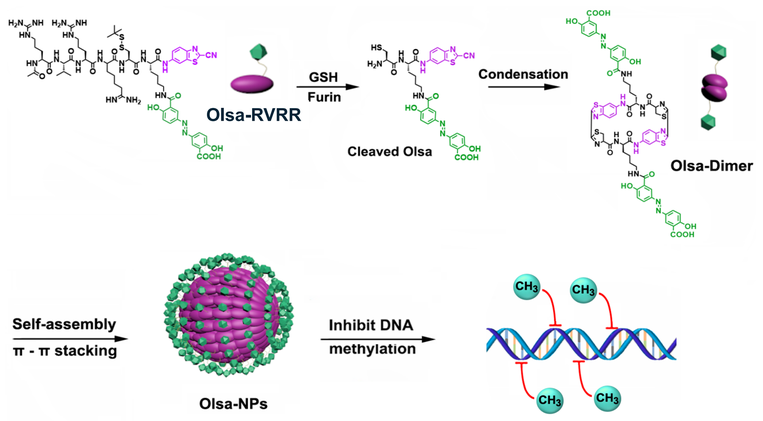

Based on a biocompatible condensation reaction recently developed by Liang and Rao et al.,[3] we designed our olsalazine derivative Olsa-RVRR with the following components: a 2-cyanobenzothiazole (CBT) motif, an olsalazine motif conjugated to the side chain of a lysine (Lys) motif, a disulfide-functionalized cysteine (Cys) motif, and a RVRR substrate for furin cleavage and improved cellular uptake of the compound. After Olsa-RVRR enters into furin-overexpressing cells (i.e. HCT 116 cells), it undergoes reduction with glutathione (GSH) and a condensation reaction controlled by furin cleavage to yield hydrophobic oligomers (mostly dimers), as demonstrated previously.[4] The oligomers then self-assemble into olsalazine nanoparticles (Olsa-NPs) at (or near) the locations of activated furin (i.e. Golgi bodies). As a consequence of their large size and hydrophobicity, which enables them to attach tightly to the membrane organelles (e.g. Golgi bodies). Hence cellular drug efflux (pump out) of Olsa-NPs is limited, prolonging their **residence** time inside cells. However, in furin low-expressing LoVo cells, with minimal cleavage of Olsa-RVRR, most of the Olsa-RVRR will remain as a monomer. The specific accumulation of Olsa-RVRR in furin high-expressing cancer cells leads to a significant amplification of CEST signal and therapeutic effects, as compared to Olsa alone (without RVRR).

In Vitro Furin Cleavage

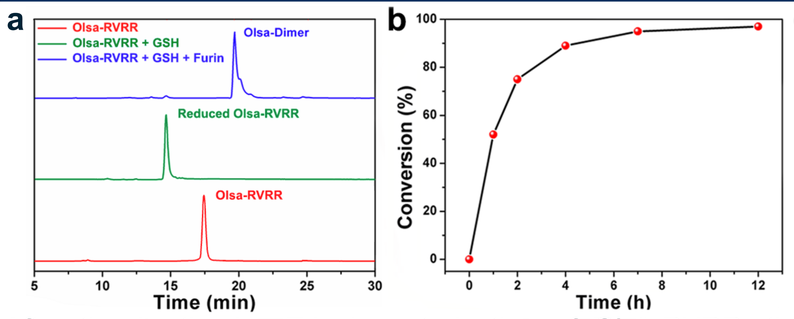

After the synthesis and characterization of Olsa-RVRR, the furin-controlled condensation of Olsa-RVRR and subsequent self-assembly of Olsa-NPs was validated. After treatment of 25 μM Olsa-RVRR with 250 μM GSH for 2 h at 37 ℃ in furin buffer, the disulfide bond of Olsa-RVRR was reduced, producing the reduction product Olsa-Red (**Fig. a**, 14.7 min at green line). After co-incubation of Olsa-RVRR with GSH and the protein convertase furin for 12 h at 37 ℃, Olsa-Red was gradually cleaved by furin to yield an active intermediate (**Fig. b**), which instantly condenses with each other to yield the hydrophobic dimer Olsa-Dimer (**Fig. a**, 19.7 min at blue line). Ultimately, the Olsa-NPs (having a diameter of 22.89 ± 3.83 nm) are self-assembled as the result of the π-π stacking interaction between Olsa-dimers, the formation of Olsa-NPs, which was confirmed by by transmission electron microscopy.

In Vitro CEST Analysis of Olsa-NPs

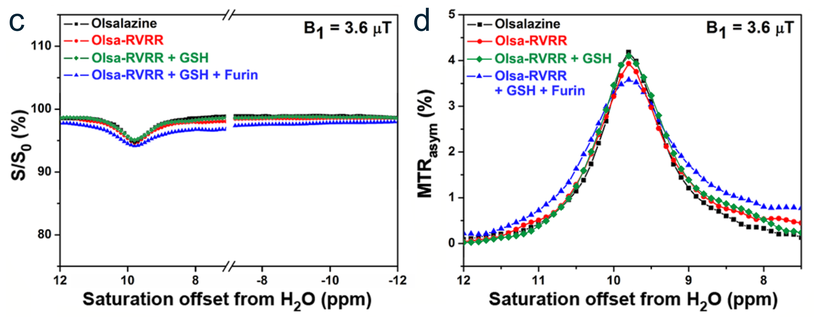

Olsa-RVRR or Olsa alone in the presence of furin was then tested for their CEST MRI contrast properties. A CEST contrast at 9.8 ppm was detected as a result from the presence of hydroxyl groups on olsalazine, similar to the chemical environment of other salicylic acids. We compared the efficacy of generating CEST signal between Olsa-RVRR and Olsa-NPs (**Figs. c,d**). The OlsaCEST signal for 5 mM Olsa-RVRR was similar to 2.5 mM Olsa alone, attributable to the 50% decrease of the number of exchangeable -OH protons for Olsa-RVRR compared to Olsa. After furin-induced condensation and self-assembly of Olsa-NPs, as demonstrated by dynamic light scattering measurements, the spectra broadened slightly, yet the intensity of OlsaCEST signal did not change significantly, indicating that most exchangeable protons remained unchanged in their interaction with water protons. Hence, modification of olsalazine and its self-assembly process does not affect the OlsaCEST signal.

In Vitro CEST MRI

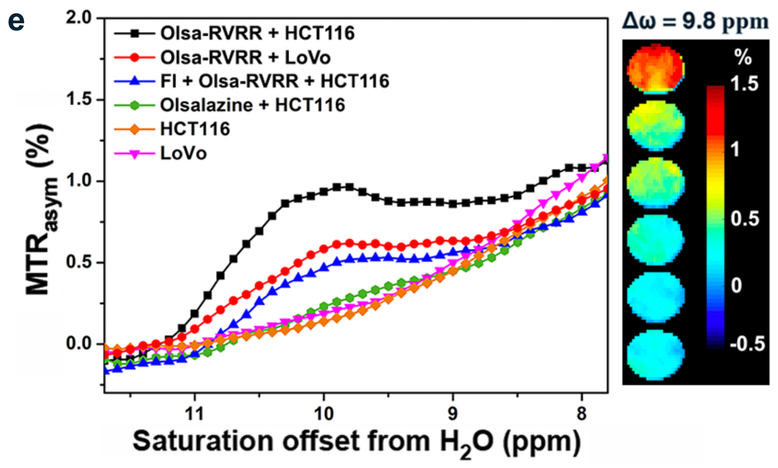

After incubation with 500 μM Olsa-RVRR for 3 h, cells were washed and collected for CEST MRI measurements. As a result of higher furin expression, HCT116 cells exhibited a 1.8-fold larger OlsaCEST signal compared to LoVo cells, resulting from the higher accumulation of olsalazine (**Fig. e**). When HCT116 cells were co-incubated with Olsa-RVRR and the furin inhibitor II hexa-D-arginine amide (FI), a 45% reduction in OlsaCEST signal was observed, providing evidence that the CEST signal is enhanced by furin-catalyzed intracellular assembly of Olsa-RVRR. To further prove that cellular penetration and intracellular nanoaggregation is essential for generating CEST contrast, HCT116 cells were incubated with 500 μM free olsazaline (without RVRR) for 3 h. The OlsaCEST signal was much lower compared to Olsa-RVRR, with no significant difference between free Olsa-incubated cells and non-incubated cells ($p>0.05$).

In Vitro Therapeutic Efficacy

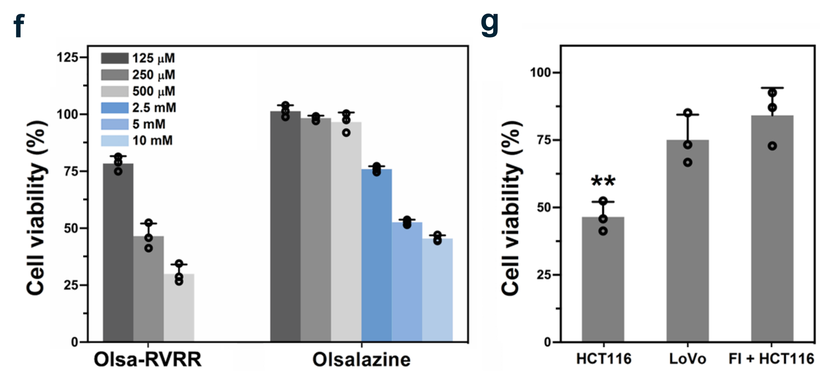

To test our hypothesis that the higher cell content of olsalazine using Olsa-RVRR is accompanied by a higher drug toxicity, we measured cell viability at 48 h post-incubation (**Fig. f**). A marked drug toxicity was observed for Olsa-RVRR at 125 μM, while for Olsa no reduced cell viability could be observed up to 500 μM; the dose needed to be increased 20-fold (2.5 mM) to obtain a comparable toxic effect. In addition, the toxicity of Olsa-RVRR towards different cells was also compared (**Fig. g**). For 250 μM Olsa-RVRR, the cell viability of HCT116 cells (46%) was significantly lower than those of LoVo cells (75%) and FI-pretreated HCT116 cells (78%) (**Fig. g**).

In Vivo CEST MRI

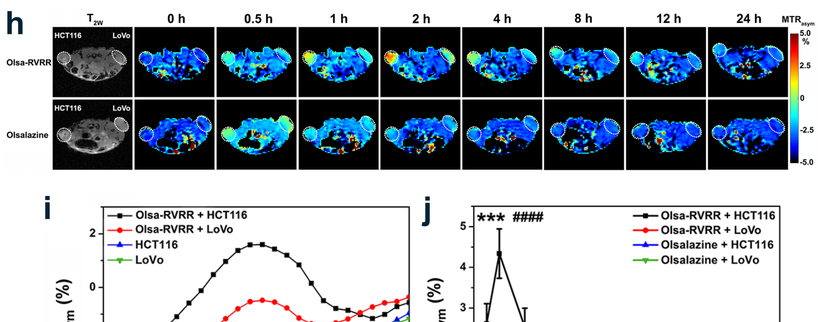

NU/J nude mice were subcutaneously (s.c.) injected with 1×10^6 HCT116 cells in the left and 1×10^6 LoVo cells in the right flank. When the tumor reached a volume of 100-200 mm^3, 0.2 mmol/kg bw (278 mg/kg) Olsa-RVRR or 0.2 mmol/kg bw (69 mg/kg) Olsa was injected intravenously (i.v.). Serial CEST MRI was obtained over 24 h to determine the time course of substrate uptake within the tumors (**Figs. h-j**). The OlsaCEST contrast was higher for HCT116 compared to LoVo for all time points. For HCT116, a maximum OlsaCEST signal increase of 4.3% was observed at 2 h post-injection (p.i.) of Olsa-RVRR, which was two-fold higher than that for the LoVo tumor (2.0%) at this time point, suggesting the accumulation of olsalazine the formation of Olsa-NPs in HCT116 tumors. In contrast to LoVo, the OlsaCEST signal could still be detected in the HCT116 tumor at 24 h p.i. For the Olsa group, no significant signal differences were detected between the tumors at any time point. Even with the two-fold higher number of exchangeable protons on Olsa compared to Olsa-RVRR, the maximum intensity observed at 0.5 h p.i. was only ~1.8%, followed by a gradual decrease at 8 h p.i., after which the signal returned to background level.

In Vivo Therapeutic Efficacy

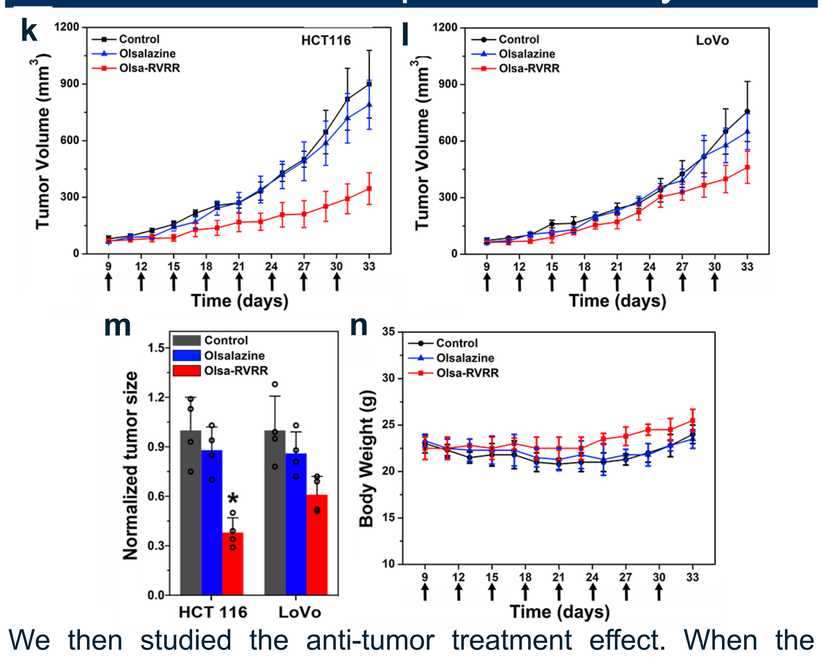

We then studied the anti-tumor treatment effect. When the tumor volumes reached 50-100 mm^3, mice were randomly divided into three groups (n=4 each). 0.1 mmol/kg bw 139 mg/kg of Olsa-RVRR, 0.1 mmol/kg bw (35 mg/kg) Olsa, and PBS were individually injected i.v. into each group. (Q3D×8). The Olsa-RVRR substrate showed a more effective inhibition of tumor growth compared to Olsa for both the HCT116 and LoVo tumor, resulting from the enhanced intracellular tumor retention of olsalazine, in agreement with the above CEST MRI results (**Figs. k-m**). Compared to the PBS control group set at 100%, at day 33 the average volume of the HCT116 and LoVo tumor reduced to ~38% and 61%, respectively, for the Olsa-RVRR-treated group, and to ~88% and 86% for the Olsa-treated group. All mice did not show any significant differences in body weight, in support of a tumor-specific toxicity (**Fig. n**).

Acknowledgements

This project was supported by the Pearl and Yueh-Heng Yang foundation.

References

[1]Bassi, D. E. et al., Mol. Carcinogen. 2001, 31, 224.
[2]Brown, W. A. et al., Digest. Dis. Sci. 2000, 45, 1578.
[3]Liang, G. et al., Nat. Chem. 2010, 2, 54.
[4]Yuan, Y. et al., Angew. Chem., Int. Ed. 2015, 54, 9700.